Energy Conversion and Management 269 (2022) 116163

Contents lists available at ScienceDirect

Energy Conversion and Management

journal homepage: www.elsevier.com/locate/enconman

A study on data-driven hybrid heating load prediction methods in low-temperature district heating: An example for nursing homes in Nordic countries

Yiyu Ding [a,*], Thomas Ohlson Timoudas [b], Qian Wang [c,d], Shuqin Chen [e], Helge Brattebø [a], Natasa Nord [a]

[a] Department of Energy and Process Engineering, Norwegian University of Science and Technology (NTNU), Trondheim 7491, Norway
[b] RISE Research Institutes of Sweden, Sweden
[c] Department of Civil and Architectural Engineering, KTH Royal Institute of Technology, Brinellvägen 23, Stockholm 100 44, Sweden
[d] Uponor AB, Hackstavägen 1, Västerås 721 32, Sweden
[e] College of Civil Engineering and Architecture, Zhejiang University, Hangzhou 310058, China

ARTICLE INFO

Keywords:
Nursing homes
District heating load prediction
Linear regression
Artificial neural network
Low-temperature district heating

ABSTRACT

In the face of green energy initiatives and progressively increasing shares of more energy-efficient buildings, there is a pressing need to transform district heating towards low-temperature district heating. The substantially lowered supply temperature of low-temperature district heating broadens the opportunities and challenges to integrate distributed renewable energy, which requires enhancement on intelligent heating load prediction. Meanwhile, to fulfill the temperature requirements for domestic hot water and space heating, separate energy conversion units on user-side, such as building-sized boosting heat pumps shall be implemented to upgrade the temperature level of the low-temperature district heating network. This study conducted hybrid heating load prediction methods with long-term and short-term prediction, and the main work consisted of four steps: (1) acquisition and processing of district heating data of 20 district heating supplied nursing homes in the Nordic climate (2016–2019); (2) long-term district heating load prediction through linear regression, energy signature curve in hourly resolution, providing an overall view and boundary conditions for the unit sizing; (3) short-term district heating load prediction through two Artificial Neural Network models, f_{72} and g_{120}, with different prediction input parameters; (4) evaluation of the predicted load profiles based on the measured data. Although the three prediction models met the quality criteria, it was found that including the historical hourly heating loads as the input to the forecasting model enhanced the prediction quality, especially for the peak load and low-mild heating season. Furthermore, a possible application of the heating load profiles was proposed by integrating two building-sized heat pumps in low-temperature district heating, which may be a promising heat supply method in low-temperature district heating.

1. Introduction

The background, literature review, and objective of this study are presented in Sections 1.1–1.3, respectively.

1.1. Background

In 2019, the building sector accounted for 35% of the global final energy use and 38% of energy-related CO_2 emissions [1]. Although there was a drop in CO_2 emissions in 2020, mainly due to the COVID-19 pandemic, the building sector's share of the final energy use and CO_2 emissions that year were 36% and 37%, respectively, almost the same as in 2019 [2].

District heating (DH) systems play a vital role in reducing primary energy use and CO_2 emissions in the building sector. In general, the primary energy factor may vary due to variation of the fuel and incentives within national policies. In the European context electricity has a primary energy factor of 2–2.5 [3], while DH of 0.6–1.3 depending on the heating sources varying from renewable-based to fossil-based fuels [4]. For example, in Sweden DH supplies 60% of the total building heating demand [5], while in Norway DH use has doubled over the past

* Corresponding author.
E-mail address: yiyu.ding@ntnu.no (Y. Ding).

https://doi.org/10.1016/j.enconman.2022.116163
Received 9 April 2022; Received in revised form 16 July 2022; Accepted 18 August 2022
Available online 27 August 2022

Nomenclature

ANN	artificial neural network
ASHRAE	American Society of Heating, Refrigerating and Air-Conditioning Engineers
CPT	changing point temperature
CV(RMSE)	coefficient of variation of the root mean squared error
DC	datacenter
DHW	domestic hot water
ES curve	energy signature curve
f_{72}	ANN model with 72 input units defined in this study
g_{120}	ANN model with 120 input units defined in this study
HDD	heating degree day
HP	heat pump
LTDH	low-temperature district heating
(s)MAPE	(symmetric) mean absolute percentage error
NMBE	normalized mean bias error
SH	space heating
WD	weekday
WE	weekend
el	electricity
€	EUR (currency)
n	number of observations
R^2	coefficient of determination
t_τ	outdoor ambient temperature at time instance τ
yr	year

decade, and currently 26.7% of DH production is used for the residential heating and 54.5% of DH production for the service heating [6]. Given the rapid electrification process in buildings, and in countries like Norway also in the transportation sector, DH has great potentials to alleviate the pressure on power grid in climates with high heating demands, such as the Nordic countries. However, DH expansion also faces two challenges, the competition from heat pumps (HPs) due to their high flexibility for the end users and consequent reduction in the final energy demand, and the decrease in the building heating demand. For the latter, this is due to the future building stock, with a growing share of renovated existing buildings, low-energy buildings, passive houses, and nearly zero energy/emission buildings (nZEB), are commonly characterized by improved building envelope, space heating (SH) demand will be greatly reduced, as noted in e.g., the Norwegian standards [7] and regulations [8], as well as the European Union's legislative framework [9]. Low-temperature DH (LTDH) enables the exploitation of economical piping options, such as PEX/Aluminum/PE material with low heat loss through distribution networks, and more importantly, provides wider opportunities for integrating distributed renewable energy, such as by use of building-sized HPs or renewables for peak shaving [10]. These advantages of the LTDH were proven in a pilot study of a renewable energy-based Danish municipality, which showed that primary energy demand was reduced by 4.5%, thermal grid loss was reduced by 6%, and costs were reduced by 2.7%, when the current 3rd generation DH system was changed to an LTDH system with the supply and return temperature of 55 and 25 °C, respectively [11].

The desire for circular economy may facilitate LTDH expansion in the Nordic countries as a result of the ban of using oil for heating [10] and increased capacity stress on the power grid due to increased power trading among neighboring countries requiring resource recovery and expansion of renewables [12]. Therefore, decreasing the DH supply temperatures from the current 80–120 °C range to a much lower level is accelerated by both political landscapes and energy efficiency directives [10]. To upgrade either the existing DH system to LTDH or build new LTDH, the change of heating load is the fundamental premise. Therefore, analyzing the potentials and challenges by understanding the key heating loads from planning and operating perspectives is the first necessary step to accelerate the LTDH transition.

A review study investigated the existing low-temperature based 5th generation district heating and cooling (LTDHC) systems in Europe, and reported that the LTDHC requires more advanced control strategies due to bi-directional energy flows and decentralized interactions [13]. Therefore, the information and communication technologies will be required to advance LTDH [13]. For example, heating and electricity load profiles on demand side may change after using power-to-heat (P2H) technologies to couple LTDH with electricity networks [14]. The change on heat and power flow may lead to operational problems and require enhanced communication between the power supply and the DH system. A control algorithm applying fuel shift control was proposed to avoid high peak power load and reduce DH network loss [14]. Another example is the need to address the impacts on DH operation network when utilizing datacenter's (DC) waste heat, e.g. due to the changing DC workload and dynamic heating load distribution, there is a need to improve DC management for automatic dynamic resources allocation, computing workloads for power management, and heating load balancing [15]. From the analysis of the challenges and potentials for LTDH in a Nordic climate, it can be seen that an LTDH system is very sensitive to the indoor set-point temperature, and it is necessary to optimize the outdoor temperature compensation curve prediction to facilitate the indoor temperature and mass flow rate [16]. Moreover, another crucial task in the LTDH system management is peak shaving, as this provides the possibility of expanding the heat network to connect more heat users without enlarging the infrastructure capacity [17]. To conclude, the above explained challenges and findings in achieving the best performance for LTDH and in establishing the feasible interaction among users; LTDH and electricity networks require intelligent prediction of peak heating load and control system, which can be adjusted by measures such as thermal storage implementation [18] and load distribution over the preceding hours [19].

1.2. Previous studies

As introduced above, LTDH and its integrations with renewables still face fundamental challenges to understand the heating load by using smart tools. Accordingly, energy prediction must be improved for effective sizing and operation of LTDH. By utilizing a large amount of measured data, data-driven methods, such as statistical methods and machine learning (ML), have shown strength in predicting heating load [20–22].

Artificial neural network (ANN), one of the ML methods, is found to be the most widely used one for energy planning, followed by support vector machine (SVM) and autoregressive integrated moving average (ARIMA) method, as well as statistical methods like linear regression (LR) [23]. A review of the last 30 years' applications of ANNs in building energy analysis shows that there is a strong growing development of ANN-based building energy analysis towards the exploitation of newer and extended types of ANNs [24]. Due to early implementation of smart meters, ANN and other data-driven methods have been mostly focused on electricity use, but not on heat use. For example, to estimate occupancy-related electricity demand by air-conditioning systems in non-residential buildings, an ANN-based model was developed by using occupancy as the input, which was determined by the blind system identification, showing an improved accuracy of energy prediction [25]. However, the proposed model needed to be validated for at least a one-year period, to account for seasonal variations of occupancy interactions with the electricity profiles [25]. Another ANN-based model compared

two back-propagation learning algorithms (Bayesian regularization and Levenberg-Marquardt), which were carried out respectively for day-ahead and hour-ahead electricity load forecast in a district [26]. Comparing with the total forecasted load for the district, aggregating the forecasts of heterogenous building types in the district may improve the day-ahead load forecasting performance by 7.9–11.9% [26]. The recent broad implementation of smart heat meters collecting (sub-)hourly heat use data has largely accelerated better quality in heating load prediction and clustering research for heating use data analysis [20]. The knowledge and experience gained from studies of building electricity demand data were transferable to heating demand analysis and uncertainties (i.e. weather forecasting), as mentioned in [27]. Two types of models, autoregressive multiple linear regression (MLR) and autoregressive multiple non-linear regression (MNLR), were firstly built to predict the DH load profiles of reference buildings and then aggregated the defined reference profiles into district levels [21]. In the work, it was shown that for predicting buildings with high daily load variation (such as office buildings), the ANN-based MNLR gives better performance than MLR in terms of a 4.2% reduction in mean squared error (MSE) [21]. Three ML methods, SVM, deep neural network (DNN, i.e. ANN with two or more hidden layers), and extreme gradient boosting (XGBoost), were respectively adopted to establish a multi-step ahead forecasting model of DH load with direct strategy and recursive strategy [22]. By feeding day-before influential factors, all three ML methods using these two strategies may accurately forecast the day-ahead DH load. Finally, it is recommended to further explore the potential of these heating load forecasting to optimize operation of the DH system [22]. Gaussian mixture model (GMM) clustering enables defining the four typical DH operation patterns in office buildings in a semi-arid climate (with cold and dry winters) by considering temperature and occupant behavior related sub-patterns [28]. After combining the GMM clustering with the regression and ANN models respectively, the qualities of hourly heating load forecasting are improved by 38.7–75.7% [28]. However, it was still difficult predicting the peak heating loads during night-to-daytime periods due to possible random operation behaviors [28]. A forecasting model based on convolutional neural network long-short term memory (CNN-LSTM) outperforms other ML methods when solving thermal inertia problems in DH system, mainly thanks to its integration of CNN's feature extraction ability and LSTM's two-dimensional space ability as shown in [29]. However, this model requires large numbers of sensors, large data storage, and re-training every day [29]. Two ML methods, SVM and nonlinear autoregressive exogenous recurrent neural network (NARX-RNN), were compared for DHC load prediction [30]. The results present that the NARX-RNN exceeds the SVM regarding the quality indicators and computation time. However, the overfitting tendency of NARX-RNN needs further study [30]. As introduced above, ANN-based prediction methods have enhanced energy prediction, especially greatly improved heating load prediction performance, such as computation time and prediction quality. However, the models' problems such as lack of big data for training, difficulty in peak load prediction, regular re-training, and others, need to be solved.

Additionally, Q-algorithm was used for developing a data-driven model by splitting the data into two parts with a reference load, $Q_{REF,}$ under three-level decision trees [27]. This model is robust for heating load prediction at district scale. Nevertheless, the claimed favorable accuracy results (R^2) in [27] are clearly lower than the common value, ca. 0.75 [31]. Based on 10-year DH production data, operation logics and outdoor temperatures were identified as the fundamental drivers for DH load prediction by analyzing load profile patterns and energy signature curves (ES curves) of the network [32]. The authors pointed out that, in the future, the parameters of a heating system should be studied according to features of each building type [32]. However, the conclusion that hourly time steps are not numerically useful is contrary to the research in [28], which presented ES curve in each cluster. Considering use of data-mining for DH operation, a temperature control method for the secondary network for transforming the existing DH to LTDH was introduced in [33]. Based on operation data and weather data, the optimized supply temperature could be obtained by summing the defined minimum return temperature and optimized temperature difference, which was evaluated by a LR model for hour-ahead return temperature prediction. This optimization strategy may contribute to stable daily operation. Meanwhile, the authors mention that this control strategy was limited within certain areas [33]. So far, only a few researchers have addressed the problems of LTDH's prediction, load analysis, and improved operation by using data-mining methods.

As the IEA DHC Annex TS2 puts forward, future decarbonized heating systems need enhanced DH technologies [10], such as installation of HPs in future's multi-energy systems [34]. This implies that shifting from competition between HPs and DH system to ensuring a collaboration between the two may be a promising approach in LTDH. An investigation of two combinations (central HPs only and central HPs plus booster HPs) for supplying space heating (SH) and domestic hot water (DHW), showed that the latter combination enables the DH system running at significantly lower temperatures and reduces operation costs by 39% over the former combination [35]. With the focus on predictions at district scale, the authors used daily average ambient air temperatures instead of hourly values [35]. This may not accommodate well for predictions at building scale, where in-depth heating response from atmospheric condition is crucial to be accounted for.

1.3. Objective and structure of this study

Previous research that focusses on improving DH system treats the measured energy data as a package, while most energy forecasts have not yet conducted in-depth studies on sizing or energy demand requirements for typical building types. Therefore, a bridge must be built to link the gap between smart meters and DH suppliers. In this study, the main objective was to develop hybrid heating energy prediction methods for typical building types, by combining the advanced ANN-based prediction method and a plant sizing method based on well-measured energy data. To focus the scope of the study, one important public building type, nursing home, was selected for the analysis. The reasons for selecting this building type and its wider applications are discussed in Section 4.1. The novel contribution of this study may be summarized as follows. Three-year measured DH use data in real buildings were utilized for analysis and modelling, which was to predict another year's DH demand in hourly resolution. The heating load profiles predicted by the hybrid methods are of high accuracy and can help plant sizing and daily operation with different inputs. Finally, the predicted load was proposed to be fed as building user's demand input in an LTDH system integrating two building-sized HPs, which may benefit the operation of building energy supply system in LTDH and compare the cost impacts from different load prediction, as discussed in Section 4.2.

The rest of the paper is organized as follows. Section 2 briefs the methods including the data information of the observed buildings and description of the two DH prediction methods. The main results of this study are presented in Section 3. Lastly, the limitations, future work, and conclusions are discussed and summarized in Sections 4 and 5.

2. Methods

The proposed framework consists of four phases. Section 2.1 explains Step 1, how building information is collected. Sections 2.2 and 2.3 explain Step 2 and Step 3, the two heating load prediction methods, dealing with the long-term and short-term prediction, respectively. Step 4 works on the prediction performance evaluation, as introduced in Section 2.4.

2.1. Building and energy data inventory

Statistically, the annual representative specific energy demand of Norwegian nursing homes is 260 kWh/m^2 with deviations between −25

and +6 kWh/m^2 according to different statistics sources, nearly half of which is for heating purpose owing to its high requirements of hygiene and thermal comfort under stable occupancy [36]. The high heating needs in the cold climates may involve considerable saving potential. In this study, 20 DH supplied nursing homes located in Trondheim, Norway, were used for the analysis. These observed buildings have heated floor areas ranging from 1350 to 10,940 m^2. DH delivers the SH and DHW to each building, which were recorded summarily in the meter. The DH use data in hourly resolution of the 20 buildings from 2016 to 2019 were retrieved from the energy monitoring platform of Trondheim Municipality [37]. Weather impacts were considered in the heat energy analysis, and the local historical weather data over the period were obtained from the Norwegian Meteorological Institute [38].

The building information regarding annual DH demand, energy labelling, and construction year, is briefed in Table 1. The building construction year and energy labelling were obtained from the Norwegian Energy Efficiency Agency (Enova) [39]. The labelling scheme goes from A (best building energy performance) to G (weakest performance) by considering the calculated delivered energy to each building. Except one building without information, all the others were built no earlier than 1980s, and most of them are labelled with C or D level [39]. The analysis was performed on the average specific DH load across the 20 buildings (W/m^2), to define the representative heating demand concerning buildings with different characteristics.

2.2. Prediction Method 1 – Prediction of annual district heating profile with energy signature curve models

As addressed above, large proportion of energy is used to heat buildings in cold climates, following the building's heating curve relative to the outdoor temperature.

In nursing homes DHW heat usage accounts for 15–20% to 40–65% of their total annual heat use, depending on the building standard (buildings built in 1980 s, passive house standard, etc.) [40]. Since DHW heat use is less sensitive to climate than SH, it is reasonable to separate DHW from the total DH load, for exploring a more accurate relationship between the outdoor temperature and the SH load. The typical per-room's hourly DHW heat use profiles for Norwegian nursing homes were identified in [41] providing detailed description and giving representative DHW profiles for the given climate and resident type. These typical hourly profiles (kW/room) were transferred into specific load density (W/m^2) and used as reference profiles in this study. As summarized in Fig. 1, there are apparent differences between the weekdays (WD as shortcut) and the weekends (WE) in the same season, especially during the peak load periods, as shown by the solid line and the dashed line of the same color. In Fig. 1, the solid lines represent the WDs, and the dashed lines the WEs. Meanwhile the seasonal differences between the same day type are small. As assumed elsewhere in literature [42], the daily DHW demand can be treated nearly constant throughout the year, and any effect on DHW would be insignificant. Similarly, in this study these four typical daily DHW profiles in Fig. 1 were extrapolated into an annual DHW profile, which was then extracted from the total DH to obtain SH use. The necessity and challenges of separating SH and DHW in the aggregated heating load was also mentioned in a Danish example for demand side management in DH networks [43].

The relationship between the outdoor temperature and SH load was identified by using energy signature curve (ES curve). This method has been widely employed in building energy planning and management by researchers and engineers at all levels. The ES curve generally consists of two parts, the temperature dependent part and temperature independent part, which are divided by the changing point temperature (CPT) or heating effective temperature. The ES curve may be expressed as:

if $t_\tau \le \mathrm{CPT}, P(t_\tau) = p_1 \bullet t_\tau + p_2 + \varepsilon$ (1).

if $t_\tau > \mathrm{CPT}, P(t_\tau) = p_1 \bullet t_\tau + p_2 + \varepsilon; = p_2$ (2).

In Eqs. (1) and (2), $P(t_\tau)$ is the SH load for a given outdoor temperature t, p_1 and p_2 are the coefficients of each ES curve model, and ε is the residual error. The SH load follows the linear growth under the slope of p_1. In addition to the outdoor temperature, the building operation schedules were also considered in the models. The identified ES curve model may be applied to estimate building energy performance in another year by combining the regression coefficients in Eqs. (1) and (2) with the corresponding weather data. Finally, Method 1 was used for the following purpose in this study: (1) for the system sizing, (2) to define boundary conditions of the DH units, and (3) to check boundary for the prediction load by Method 2.

2.3. Prediction Method 2 – Artificial neural network short-term district heating prediction

In this study, day-ahead prediction refers to the problem of, at a given point in time, predicting the DH load for the following 24-hour period. This prediction was done with an hourly resolution. Two separate ANN prediction models were developed to serve as decision-supporting tools for short-term planning and operation purposes in the future LTDH transitions. The first model considered only the historical and forecasted outdoor temperature, which are the measured outdoor temperature for the 48 h preceding the prediction period plus the 24-hour forecast for outdoor temperature. The second model included the historical DH load, the measured DH load for the 48 h preceding the prediction period, in addition to the outdoor temperature used in the first model. The first model might be helpful when there is difficulty to access real-time energy data or when data storage failure occurs with many missing values for planning energy generation.

The two models can be mathematically formulated as follows: Q_τ and t_τ represent the measured DH load and the measured outdoor temperature, at hour τ, respectively; and $\widehat{Q}_{\tau,s}$ and $\widehat{t}_{\tau,s}$ represent the predicted DH load and the forecasted outdoor temperature, respectively, at hour τ for each of the hours $\tau+s$ (defined for $s = 1,\cdots,24$). Historical data from the previous 48 h were used to make the prediction as the following:

$$\widehat{Q}_\tau^{24} = \left(\widehat{Q}_{\tau,1}, \cdots, \widehat{Q}_{\tau,24}\right), \tag{3}$$

$$\widehat{t}_\tau^{24} = \left(\widehat{t}_{\tau,1}, \cdots, \widehat{t}_{\tau,24}\right), \tag{4}$$

$$Q_\tau^{48} = (Q_{\tau-48+1}, \cdots, Q_\tau), \text{ and} \tag{5}$$

$$t_\tau^{48} = (t_{\tau-48+1}, \cdots, t_\tau) \tag{6}$$

where Q_τ^{48} and $\widehat{Q}_\tau^{24}$ represent, at hour τ, the historical measured DH load for the previous 48 h (including τ) and the predicted DH load for the next 24 h, respectively. Similarly, t_τ^{48} and $\widehat{t}_\tau^{24}$ represent, at hour τ, the historical measured outdoor temperature for the previous 48 h (including

Table 1
List of observed buildings' information.

Average measured annual DH demand (kWh/m^2)	≤70	≤90	≤120	≤160	≤190	>190	
No. of buildings	/	7	6	6	1	/	
Energy labelling with maximum	A	B	C	D	E	F, G	No infor.
Delivered annual energy (kWh/m^2)	140	190	240	295	355	440, >440	
No. of buildings	/	4	6	6	3	/	1
Construction year	Before 1950	1950–1979	1980–1999	2000–2010	After 2010		No infor.
No. of buildings	/	/	7	9	3		1

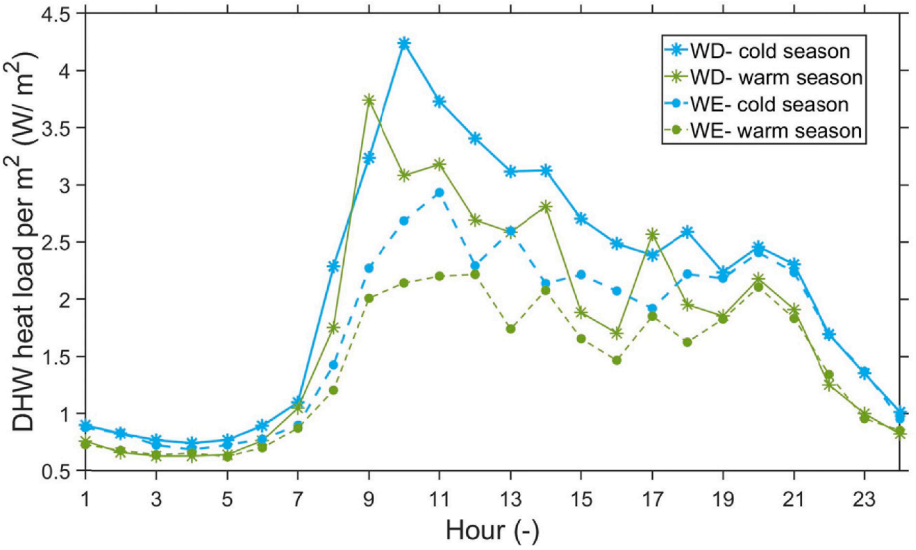

Fig. 1. Daily DHW heat load profiles in the nursing homes, divided by day of week and seasons.

τ) and the predicted outdoor temperature for the next 24 h, respectively. Using these notations, the two models could be expressed mathematically as:

$$\text{if historical heating load is not an input to the model, } \widehat{Q}_{\tau}^{24} = f\left(\widehat{t}_{\tau}^{24}, t_{\tau}^{48}\right), \tag{7}$$

$$\text{if historical heating load is an input to the model, } \widehat{Q}_{\tau}^{24} = g\left(\widehat{t}_{\tau}^{24}, t_{\tau}^{48}, Q_{\tau}^{48}\right) \tag{8}$$

where f and g are the abstract representations of the two ANN prediction models. Eq. (7) presents the first model considering outdoor temperature as the predictor, while Eq. (8) presents the second model considering both outdoor temperature and DH load as the predictors.

Both ANN models were established with one input layer (the first model, f, with 72 input units, and the second model, g, with 120 units), one hidden Rectified Linear Unit (ReLU) layer with 64 nodes and one output layer. 64 nodes were determined through hyperparameter search. For simplicity, notation f_{72} represents model $f\left(\widehat{t}_{\tau}^{24}, t_{\tau}^{48}\right)$ in Eq. (7) and notation g_{120} represents model $g\left(\widehat{t}_{\tau}^{24}, t_{\tau}^{48}, Q_{\tau}^{48}\right)$ in Eq. (8). These two notations are used in the following text. All the layers are densely connected. Mean squared error (MSE) was used as the loss function, and *Adam* was used for the parameter optimization with the maximum number of epochs at 100. The models were originally tested with 24, 48, and 72 h of historical data (weather and/or DH load). It was found that the difference between using 48 and 72 h of historical data was not significant while between using 24 and 48 h was significant, regarding the loss function. 48-hour historical data were therefore chosen due to the faster speed of running the models. The datasets of 2016 and 2017 were used as the training set establishing the ANN model, and the dataset for 2018 were used as the validation dataset for assessing the model performance during building and tuning the model process. To examine whether the model overfits the training set and is capable for future deployment, the resulting models were used to predict the DH load profile for 2019 and the prediction quality was evaluated using the measured data for the entire 2019, which was an unseen dataset during modelling process.

2.4. Evaluation of the prediction performance

Quality of the prediction models was evaluated by the commonly used criteria: mean absolute percentage error (MAPE), normalized mean bias error (NMBE), and the coefficient of variation of the root mean squared error (CV(RMSE)); meanwhile symmetric mean absolute percentage error (sMAPE) was also used as a supplementary criterion of MAPE, with lower and upper bounds. MAPE summarizes the relative error between the actual and predicted use in absolute value with a division by the observation number n. The directionality of the NMBE implies whether there is over-prediction or under-prediction. CV(RMSE) indicates whether the predicted model can reflect the real load shape. The criteria NMBE and CV(RMSE) shall be no more than 10% and 30%, respectively, when analysis is on hourly basis, according to the ASHRAE guidelines [31,44], while the MAPE shall be no more than 20% for a good forecasting model [45].

MAPE was given as:

$$MAPE = \frac{1}{n}\sum_{i=1}^{n}\left|\frac{A_i - F_i}{A_i}\right| \bullet 100\% \tag{9}$$

sMAPE was given as:

$$sMAPE = \frac{1}{n}\sum_{i=1}^{n}\frac{\lceil A_i - F_i \rceil}{(\lceil A_i \rceil + \lceil F_i \rceil)/2} \bullet 100\% \tag{10}$$

NMBE was given as:

$$NMBE = \frac{1}{n}\frac{\sum_{i=1}^{n}(A_i - F_i)}{\overline{A}} \bullet 100\% \tag{11}$$

CV(RMSE) was given as:

$$CV(RMSE) = \frac{\sqrt{\frac{1}{n}\sum_{i=1}^{n}(A_i - F_i)^2}}{\overline{A}} \bullet 100\% \tag{12}$$

where A_i is the measured value, F_i is the predicted value, and n is the number of the observations.

3. Results

The daily SH profiles, analysis results of the ES curve model, and the predicted annual DH profiles are presented in Sections 3.1 and 3.2. The 24-hour period prediction results for the warm and cold seasons are presented in Section 3.3. Lastly, the prediction performance is evaluated in Section 3.4.

3.1. Average daily space heating profiles and heating degree day results

After removing the daily DHW heat use in Fig. 1, the average daily SH load profiles for the nursing homes 2016–2018 were made by using arithmetic mean value of each hour, as shown in Fig. 2. This was to

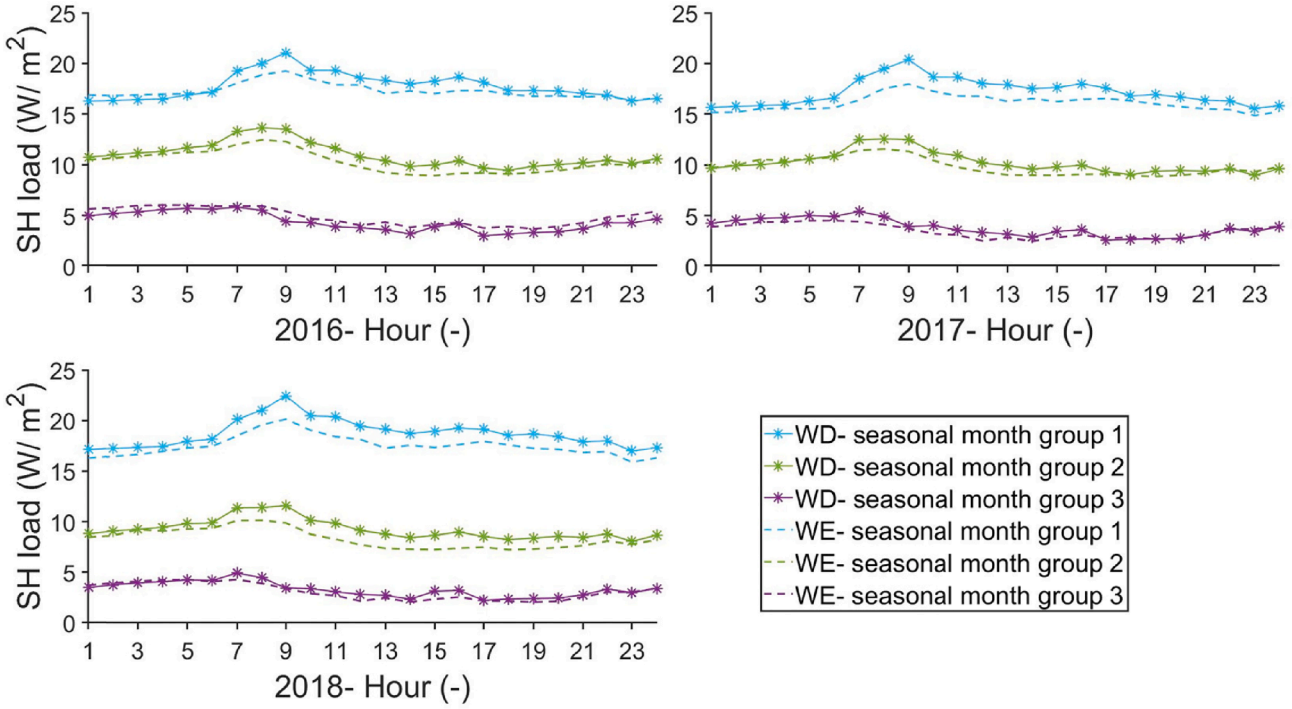

Fig. 2. Average daily SH load profiles 2016–2018, considering three seasonal month groups.

compare the load profiles between seasons and day types in general. In Fig. 2, the solid lines with stars and the dashed lines represent weekdays (WD) and weekends (WE), respectively.

The seasonal month group 1 included November – March, the seasonal month group 2 included April, May, September and October, and the seasonal month group 3 included June, July and August. Among the three seasonal groups, the heating load generally arose between 6 o'clock and 16–17 o'clock with the peak load at around 9 o'clock, which could be noted on weekdays, weekends, and short holidays. This is in line with the survey that most of the nursing homes take their main daily activities such as medical treatment, health training, and reading, between 7 and 16 o'clock, when large SH demand is needed in common areas. Due to stable occupancy of patients and residents, the heating load profiles for nursing homes demonstrate a milder peak load during the working hours and relatively higher level during the non-working hours in nursing homes, comparing with the buildings featured with distinct night setback control operation and different attendance levels between the weekdays and the weekends, such as educational buildings, office buildings, and other administrative buildings [46,47].

Further, to see whether day types might affect SH use, the obtained SH use was segregated into four heating seasons by using the heating degree days (HDDs) [48,49]. HDD was calculated as the daily average difference between heating balance temperature t_{bal} and hourly outdoor temperature: $\frac{1}{24}\sum_{\tau=1}^{24}(t_{bal}-t_{\tau})$, by assuming t_{bal} at 15 °C and setting negative values to zero. Days with HDD lower than $\frac{5}{24}$°C were considered as summer, between $\frac{5}{24}$ and $\frac{100}{24}$°C as the transition season, between $\frac{100}{24}$ and $\frac{510}{24}$°C as the heating season, and with over $\frac{510}{24}$°C as the very cold season. As shown in Fig. 3, it can be concluded that the daily SH operation generally follows the daily HDD closely, without influence of the

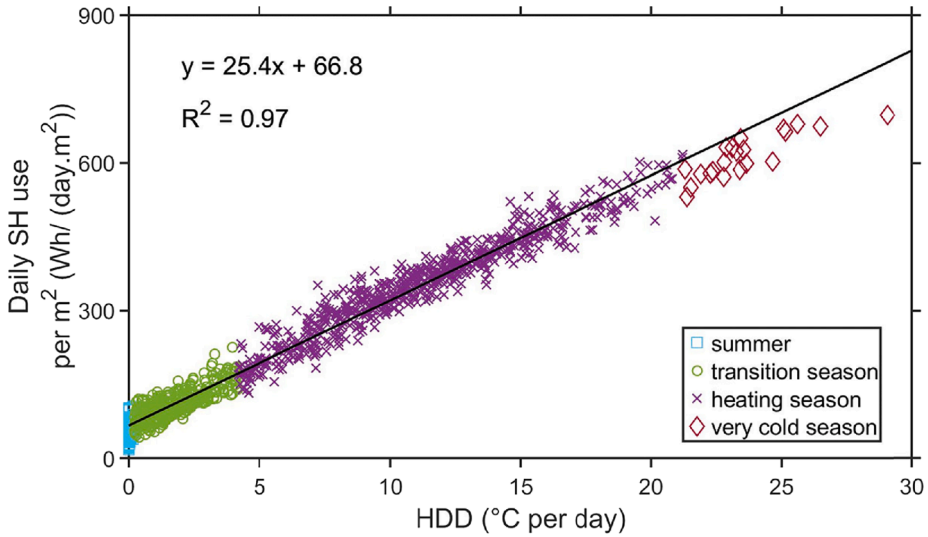

Fig. 3. Daily SH use vs. daily HDD, based on four different heating seasons, summer, transition season, heating season, and very cold season (high-heating season).

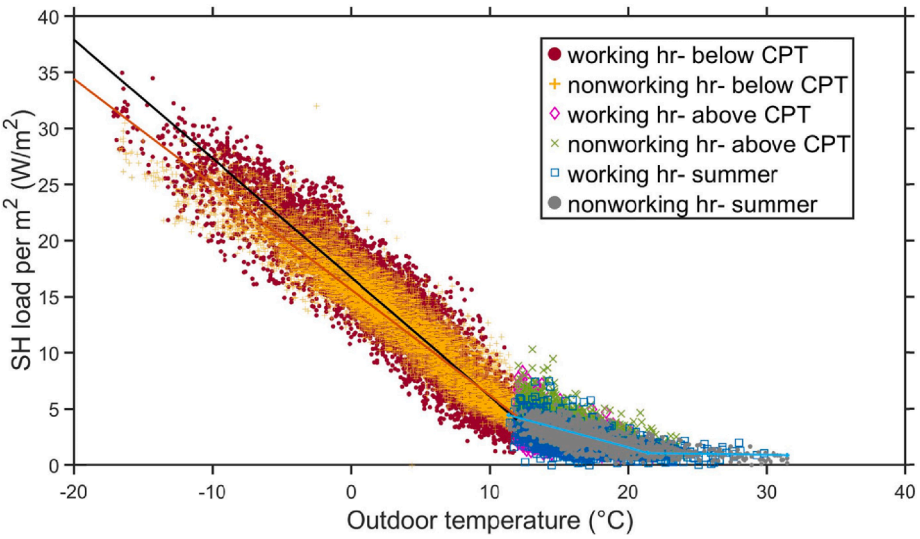

Fig. 4. Energy signature curve models of SH load. The black line below CPT represents working hours and red line non-working hours.

day type (weekday or weekend) nor manual false operation. Therefore, the ES curve models for SH prediction were established based on working hours and non-working hours, respectively, by following Eqs. (1) and (2).

3.2. Energy signature curve model and annual district heating profile

The ES curve models for the SH load are presented in Fig. 4, where the CPT was found at around 12 °C for providing a proper piece-wise approximation. The outdoor temperatures above the CPT covered 22.4% of the entire heating periods, when the SH loads were less temperature dependent as shown under the mild and constant slope. These small loads could be described by one regression line regardless of working hours and non-working hours. The remaining 77.6% of the time, the outdoor temperatures were below the CPT, falling into high-heating season. Along the regression lines below the CPT, there was a small region where non-working hours might need a slightly higher SH load than working hours under the same outdoor temperature (ca. 10–12 °C). This might be explained by residents spending more time outdoor during working hours at higher outdoor temperatures, causing the ventilation heat demand to decrease slightly due to changes in occupancy. The quality of regression models was evaluated with the coefficients of determination R^2, and the results are given in Table 2, together with the coefficients for the ES curves.

In Table 2, for the outdoor temperatures lower than CPT, it might be noted that R^2 were much higher than the required 0.75 for achieving a satisfying regression model [31,44]. However, for the part above the CPT, the SH needs had minor impacts on energy system requiring small load within short duration time. Comparing with those buildings with distinct time clock control operation, there were not pronounced SH differences between the working and the non-working hour periods in nursing homes, it is still worth analyzing them separately.

By using Method 1 introduced in Section 2.2, the reversely predicted annual DH profile of 2016–2018 was compared with each year's measured DH profile in Fig. 5. It can be observed that the DH load had large seasonal variation with the peak load during winter and early spring, and most of the predicted DH loads (green lines) were close to the measured DH loads (red lines). The annual DH demand of the three years were around 111–113 kWh/m^2 with peak SH load 31–35 W/m^2. By using the coefficients and knowledge obtained from the three years, the annual DH profile for 2019 was predicted, as shown in Fig. 6 giving a breakdown of the SH and DHW heat load profile. The peak SH load was 29–31 W/m^2 at outdoor temperature of −11.6 to −9.3 °C and the minimum load was close to 0.9 W/m^2 for the network circulation, while the DHW use was considered process heat with seasonally stable usage patterns. The predicted annual total DH demand for 2019 was 114 kWh/m^2, 15% of which was for DHW heat use. The results follow the statistical data of heat use in nursing home including the share for DHW heat use [40]. From this, a typical nursing home with an average area of 7000 m^2 may need around 800 MWh energy for heating purpose annually with a peak SH load of 203–245 kW under the similar climate. This also provides the boundary conditions that the day-ahead predictions shall be constrained by the operation scenarios, instead of allowing the network temperature drift freely with load variations.

Table 2
Coefficients of Eqs. (1) and (2), and the corresponding R^2.

	Outdoor temperature dependent ≤ 12 °C		Outdoor temperature less dependent	
	Working hour	Non-working hour	13–20 °C	>20 °C
p_1	−1.1	−0.94	−0.3	/
p_2	16.7	15.9	8.0	0.9
R^2	0.89	0.90	0.37 (↓)	

3.3. Results of short-term district heating load prediction

The day-ahead prediction performance of the two models f_{72}, g_{120} are compared in Fig. 7 and Fig. 8, and examples from different heating seasons were selected. To recall, model f_{72} did not consider the historical DH load as input, whereas g_{120} did consider the historical DH load, as stated in Section 2.3. In both models, the next 24-hour heating load prediction for the whole year of 2019 was made from 0 o'clock (τ) on January 1 to 0 o'clock (τ) on December 31 and gave 8737 prediction results in total, respectively.[1]

In Figs. 7 and 8, the top row subplots show the prediction results for f_{72}, and the bottom row subplots the results for g_{120}. Each column subplot shows the prediction for the next 24-hour period following the time instance indicated at the top, e.g., the prediction of the heating load $\widehat{Q}_\tau = (\widehat{Q}_{\tau,1}, \cdots, \widehat{Q}_{\tau,24})$ is plotted for the τ on the given date. By looking at each column subplots, it is therefore easy to compare the performance of

[1] Since weather of 2020 was not included, the prediction finished at 0 o'clock (τ) on December 31 with weather input by 23 o'clock on December 31. Therefore, each model ran 8737 times prediction (excluding 1–23o'clock (τ) on December 31) and produced 8737 prediction results, respectively.

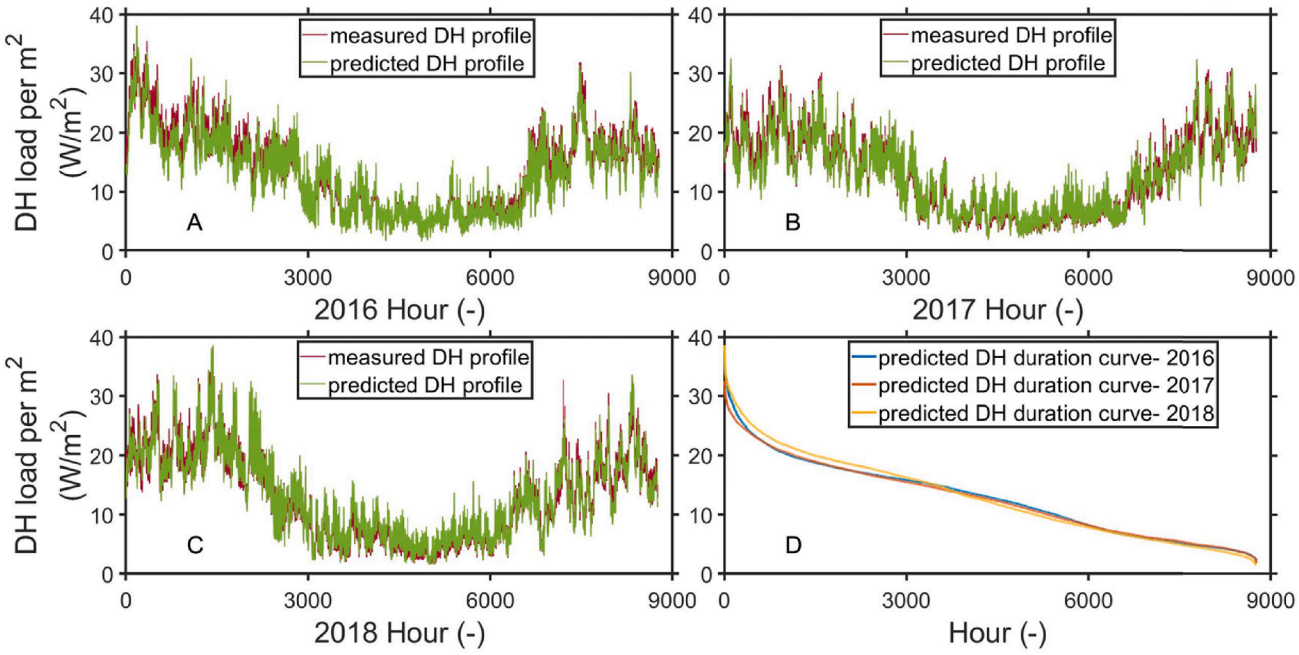

Fig. 5. Measured vs. predicted DH load profile during 2016–2018 (subplot A–C), and predicted DH duration curves during 2016–2018 (subplot D).

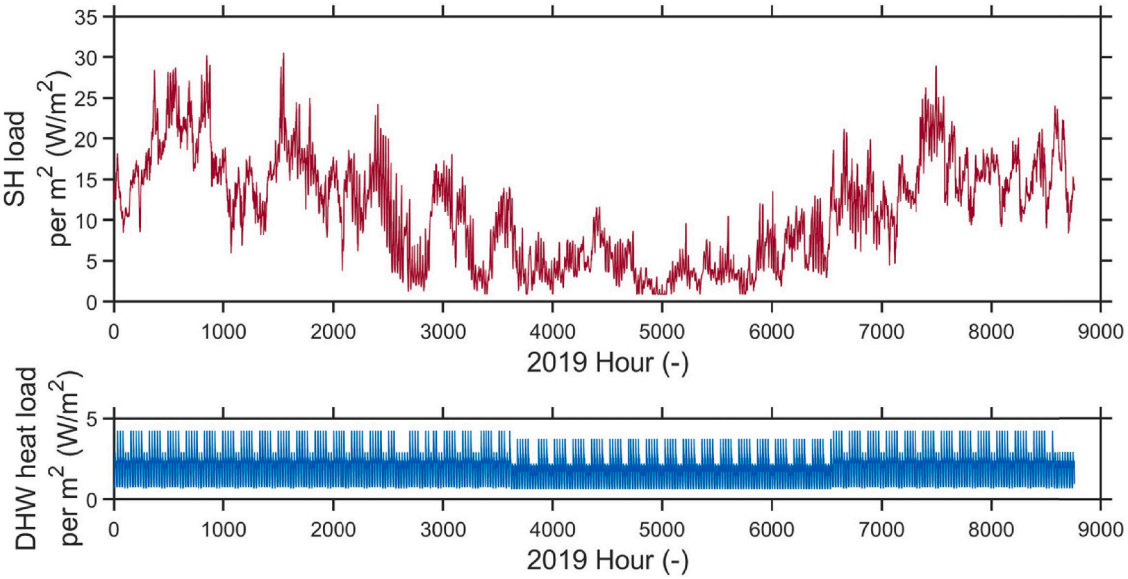

Fig. 6. Predicted DH load profile for 2019 with a breakdown of SH load profile (top row subplot) and DHW heating load profile (bottom row subplot).

model f_{72} and model g_{120} for the same time instance. In Figs. 7 and 8, the dashed black line represents the forecasted outdoor temperature for the corresponding 24-hour period, which are the actual outdoor temperature and used for evaluation in this case. To hold statistical reliability, three prediction results out of the 8737 instance τ were randomly selected from the 2019 testing data using a uniform probability distribution. The sample results are presented in Fig. 7, in which there were two DH load spikes, one was measured at 9 o'clock on September 16 and the other one at 3 o'clock on October 27, see the green squares pointed by the gray arrows. Since the first random samples were not part of the (high-) heating season (cold period with high heating demand), further, the prediction results for three dates during January, February, and December were randomly selected, covering the outdoor temperature from −11 to 2 °C, as shown in Fig. 8. In all the seasons, the load predicted by model g_{120} was apparently closer to the measured load than the one predicted by model f_{72}, both to the curve patterns and load values.

3.4. Results of the prediction performance evaluation

Due to thermal and hydraulic inertia in DH systems, and energy source availability, daily operation is commonly planned and arranged based on energy demand prediction for satisfying end-users' heating need in an economical way. By accumulating the daily prediction from Method 2 introduced in Section 2.3, a summed deviation between the predicted and the measured data throughout a year may be visualized. The deviation accumulated during (high-) heating season is especially important for evaluating peak loads prediction performance. Since the models, f_{72} and g_{120}, respectively produced next 24-hour heating load prediction at (any) hour τ, it is possible to select the same hour τ of each

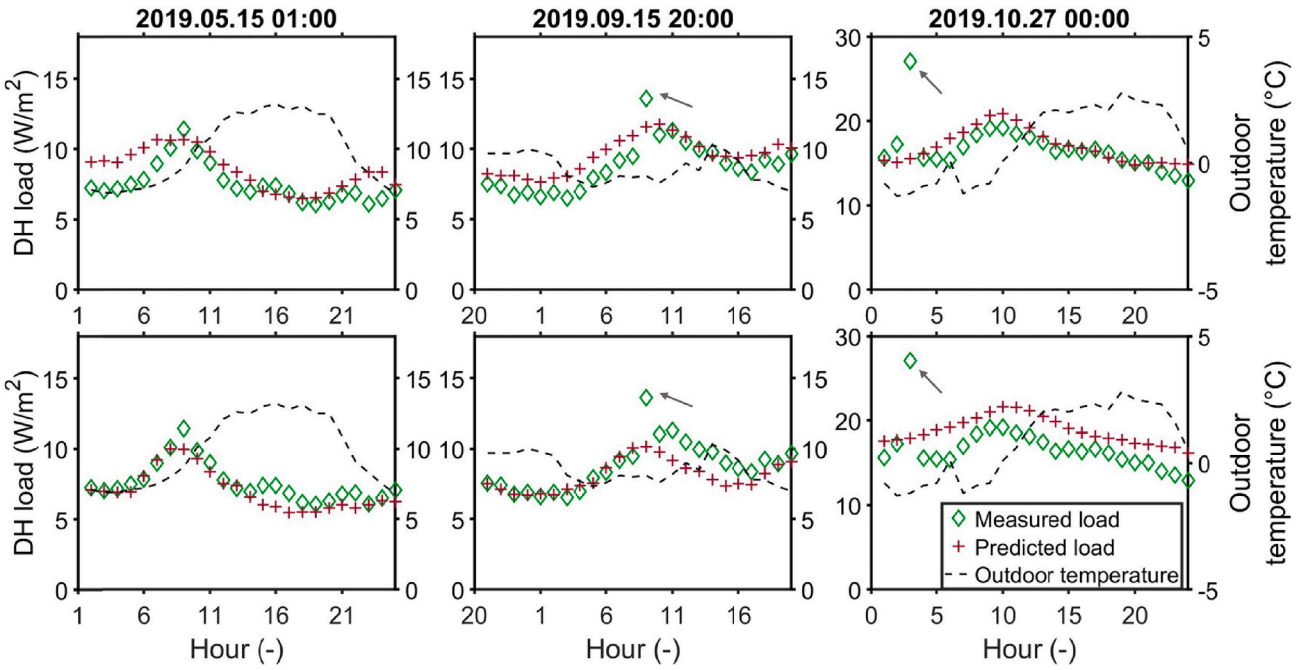

Fig. 7. Predicted DH load for the 24-hour period following the date indicated above each column, showing the randomly selected prediction results by model f_{72} (top row subplots) and by model g_{120} (bottom row subplots).

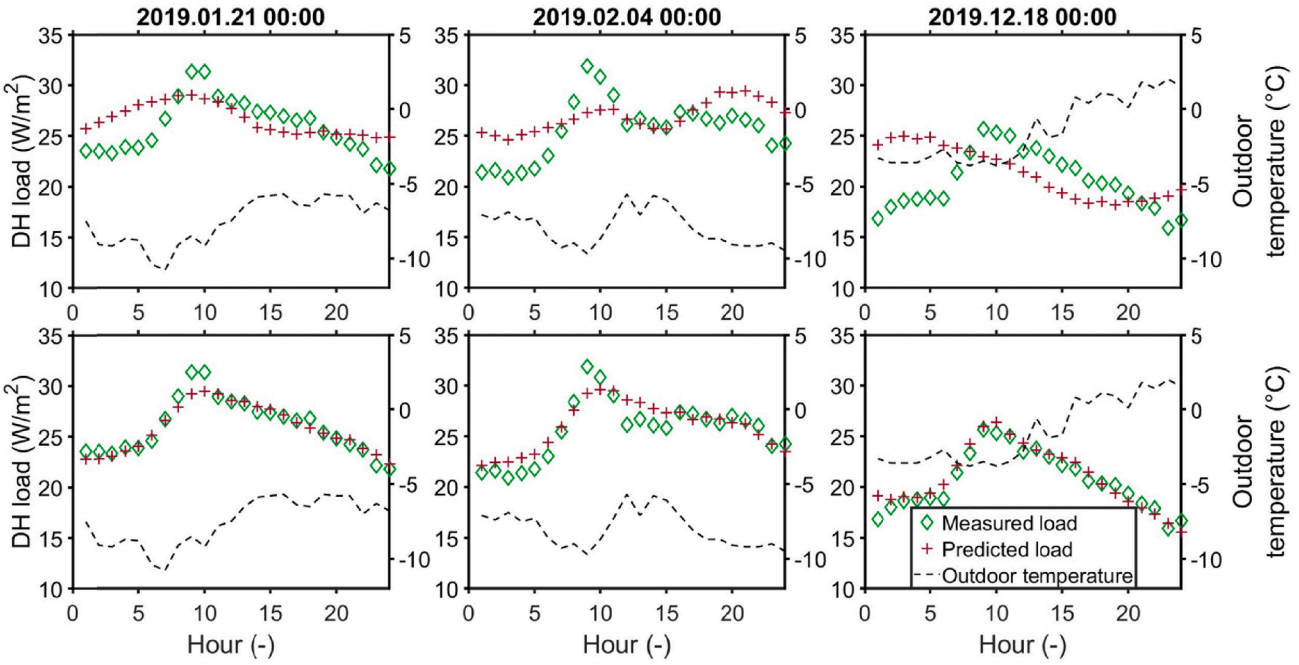

Fig. 8. Predicted DH load for the 24-hour period following the date indicated above each column, showing the selected three dates prediction results by model f_{72} (top row subplots) and by model g_{120} (bottom row subplots).

day for planning the next-day's production. Accordingly, the 24-hour ahead prediction results made at 0 o'clock every day from January 1 to December 31 were accumulated for obtaining the annual predicted load profile for 2019. It shall be noted that these accumulated annual profiles were obtained differently than the one presented in Section 3.2, which was made by Method 1, the ES curve model – directly on a long-term basis.

Fig. 9 compares the predicted load profiles for 2019 made by Method 1- ES curve model (the green line), Method 2, model f_{72} (the dark red line), and model g_{120} (the yellow line), with the measured load profile (the blue line). The deviation between the measured load and the predicted load, $\Delta(\tau) = measured\ \ Q_\tau - predicted\ \ \widehat{Q_\tau}$, by the three models for 2019 are shown in Fig. 10, and the prediction accuracy evaluation of the three models is summarized in Table 3. In Fig. 9 all the three predicted load profiles followed seasonal variations, and the profiles by models f_{72} and g_{120} fell within the sizing boundary set by Method 1. g_{120} demonstrated an advantage in predicting heating load in mild- and low-heating seasons, during which most of the heating needs were DHW use and therefore had a weak linear relationship with the outdoor

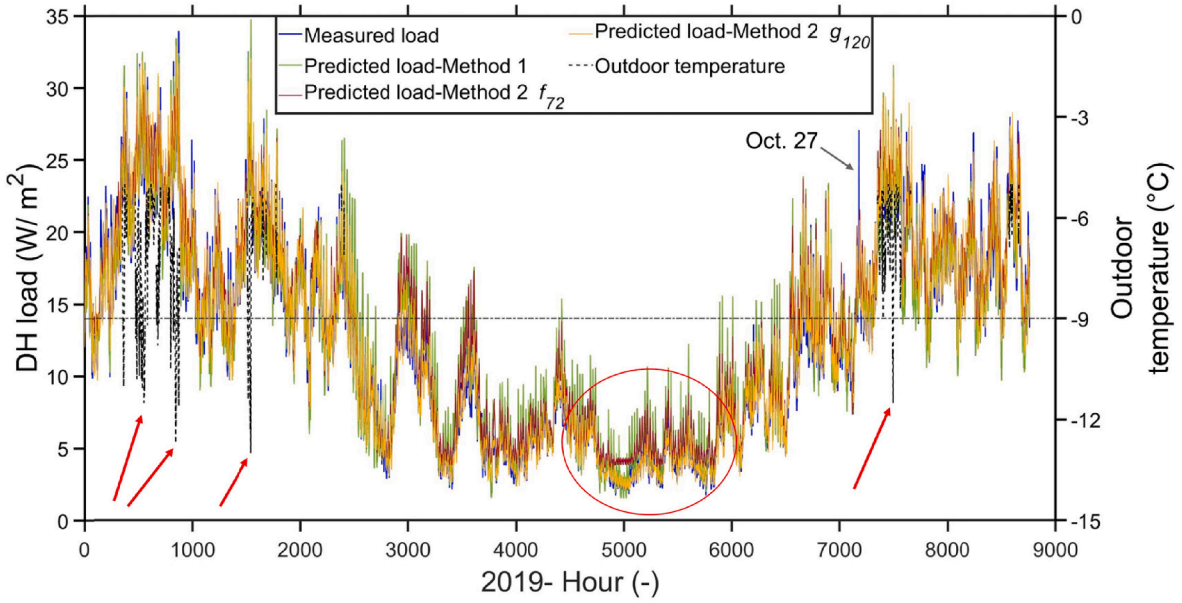

Fig. 9. Measured vs. predicted annual DH load profiles by the three models for 2019.

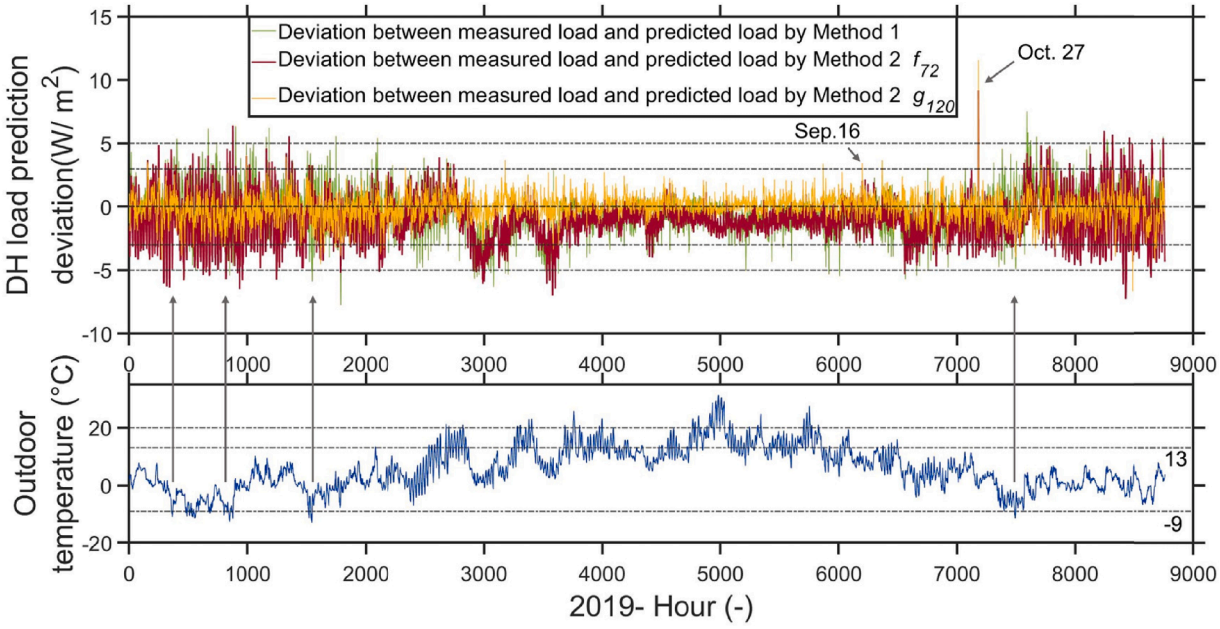

Fig. 10. Deviation plot between measured and predicted DH load by the three models for 2019.

Table 3
Evaluation results of 2019 DH load forecast produced by the three models. The criteria, MAPE, sMAPE, NMBE, and CV(RMSE), are used for quality evaluation.

Prediction method	MAPE (%)	sMAPE (%)	NMBE (%)	CV(RMSE) (%)
Method 1-ES curve model	13.94	12.81	−3.91	13.79
Method 2-model f_{72}	16.77	14.75	−8.13	15.51
Method 2-model g_{120}	7.23	7.28	−0.36	7.90

temperatures, as indicated by the red circle. In Fig. 9, the horizontal dash-dotted line refers to the reference line of the outdoor temperature at −9 °C, and only outdoor temperatures below −5 °C are presented as shown in the black dashed line; the red arrows point to the four examples of the peak heating load periods, as presented in Fig. 11. As compared in Fig. 10, g_{120} held the prediction deviations within ±3 W/m^2 during most of the time, f_{72} had highest deviations during cold periods either over-predicting DH load or under-predicting DH load, and the ES curve kept the prediction deviation in between. The deviation high spikes on October 27 were mostly caused by measurement failure, see Fig. 7, when a sudden high DH load was measured.

In Fig. 11, Model f_{72} was least sensitive to the outdoor temperature changes by underpredicting the peak load and overpredicting the load during other time, also seen in Fig. 10; the ES curve model and model g_{120} catch most of the peak load periods, whereas the ES curve model might have overpredicted the peak load and caused unnecessary costs comparing to g_{120}. To recall Fig. 3, the regression line generally correlated well between the daily HDDs and the daily SH demand, however it might have overpredicted the SH use in the short and very cold season.

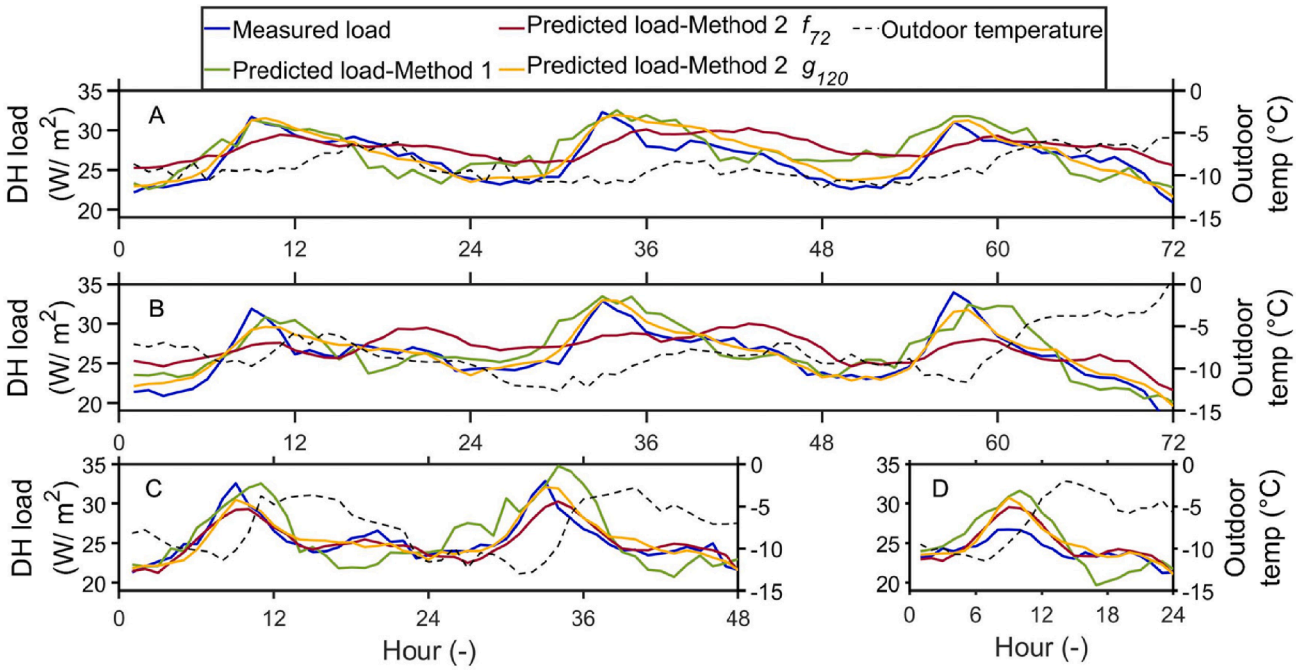

Fig. 11. Four examples of peak load periods in 2019, measured vs. predicted DH profiles by the three prediction models. Subplot A represents the load profiles comparison from 1 o'clock on January 22 to 24 o'clock on January 24. Subplot B represents the load profiles comparison from 1o'clock on February 4 to 24 o'clock on February 6. Subplot C represents the load profiles comparison from 1 o'clock on March 5 to 24o'clock on March 6. Subplot D represents the load profiles comparison from 1 o'clock to 24 o'clock on November 9.

Since the ES curve model below the CPT was determined by considering heating season and very cold season together, this might explain the possible overprediction of the peak SH load by Method 1.

As listed in Table 3, the MAPE and sMAPE results of the three models were less than 20%, NMBE within ±10%, and CV less than 20%, meeting the criteria upper limits [31,44,45]. Despite using the same training set for f_{72} and g_{120}, g_{120} had the best prediction performance on a yearly basis benefitting from using both the nearest historical two-day heating load and the outdoor temperatures as inputs, while f_{72} only considered the ambient condition as the inputs and its prediction accuracy was reflected by the poorest results regarding all the criteria. However, it was still good to notice that the load predicted by f_{72} to some extent was able to catch the pattern from the measured load curves, even without historical DH load as inputs, as reflected by its criterion CV (RMSE) result, much lower than the limit, 30%. Besides setting load boundary, the heating load prediction quality of the ES curve model was in the middle of the three models.

This means the models and their predicted DH load profiles provided high accuracy for use in the following work, regardless of the different input settings and algorithms of the three prediction models.

4. Discussions and future study

Selection of the analyzed building type data is reasoned in Section 4.1. Section 4.2 discusses three points, rationality of the models, limitation, and future work. The value of transferring this work is presented in Section 4.3.

4.1. Rationale of building type data inventory

A selection of nursing homes in the city of Trondheim was selected for the data analysis and modelling. A modern nursing home covers a large floor area and includes residents' private rooms with round-the-clock occupancies, large common area, 24/7 nursing service, and administrative offices. In 2018, the Norwegian long-term care expenditure accounted for 3.5% of GDP, while the average expenditure in OECD countries was 1.5% [50]. The function and characteristics of this building type make it an important public residential building with respect to social welfare progress and residents' care needs in the aging society.

The energy use in special residential building types, such as nursing homes, has more true-needs for users during whole heating seasons, and has not yet been extensively studied compared to residential buildings, especially in the cold climate, as mentioned in [41]. Since most of them are supplied by DH, it is important to study their energy needs in the transition to LTDH and to improve building energy supply, and for this, it is important to develop reliable prediction methods.

4.2. Discussions

4.2.1. Rationality of the models

By making good use of big data, data-driven models were selected over physical models. In Fig. 7, there were two DH load spikes, whereas the load profiles predicted by the two ANN models demonstrated a smoother trend. After checking the outdoor temperature during the two days, no "sudden" weather changes were recorded. Thus, these unusual data values might have been caused by metering failures or false operation. Nonetheless, the established models showed more reasonable heating load prediction. Besides the proper algorithms, the three-year's large data for training/validation also contributed to the appropriate prediction.

4.2.2. Limitation

The models adopted the actual measured outdoor temperature (the predictor) as the forecasted outdoor temperature for prediction. Practically, this weather forecast would however be inaccurate to some extent and may consequently cause a weaker performance than the observed in this study. Therefore, it is important to build the base model as accurately as possible, to reduce the spread and impacts of such weather uncertainties and inaccuracies. Meanwhile, due to this study's limited scope and length, only the hybrid of a linear regression model and an ANN model was considered. Although the prediction results were

satisfactory, a further study shall investigate whether there are other types of prediction methods, and newer types of ANN architectures may achieve better results, even with less training data available.

4.2.3. Future work – integration of building sized heat pumps in low-temperature district heating

In addition to improving DH load prediction quality, the above-described heating load profiles for DHW and SH may be utilized respectively in building energy supply operation when the building is connected into LTDH system. For example, it would be helpful to respond the different minimum allowable supply temperature requirements of DHW and SH by integrating two building-sized boosting HPs in LTDH. This may be regarded as a promising solution towards one of the challenges in LTDH. One possible application may be proposed as shown in Fig. 12, where from left to right side are the emerging heat source from waste heat, the temperature upgrade process, and the building user.

According to the Norwegian regulation, when a water storage tank is included, the DHW temperature should be maintained at not lower than 65 °C to prevent Legionella's growth [51]. One booster HP (HP1) may be accordingly employed for upgrading the heat source temperature e.g., from 55 to 65 °C for DHW heating, which connects to a water storage tank and a heat exchanger at substation.

The second booster HP (HP2) may be employed for upgrading the heat source for satisfying the peak SH load, when the outdoor temperature reaches a critical point that the source temperature is unable to maintain thermal comfort. For example, when using the conventional radiators in Nordic housings, the critical point may be determined as in [52] giving the equation as:

$$t_{in} = -0.75 \bullet t_{\tau} + 51 \tag{13}$$

where t_{τ} is the outdoor temperature and t_{in} is the minimum heating supply temperature. Additionally, selection of the critical point shall also consider the energy system's flexibility and use of building thermal inertia as shown elsewhere [53,54].

When the HPs or other boosting units are electric-driven, the annual electricity bill for heat source upgrade process is calculated by summarizing the monthly cost, which may follow Eq. (14):

$$C_{mon} = (1 + 0.25) \bullet \sum_{t=1}^{720or744} v_{\tau} \bullet \dot{E}_{\tau} + f \bullet \sum_{t=1}^{720or744} \dot{E}_{\tau} + \frac{F}{12} \tag{14}$$

where τ is the time instance, 0.25 is the tax rate on spot price, v_{τ} is the variable power market price, considered with the NordPool spot price of Trondheim in 2019 [55], $\dot{E}_{\tau}$ is the hourly electricity use, f is the grid rent with a value of 0.023€/kWh, and F is the fixed annual fee with a value of 190€/yr to ensure customers' access to electricity covering the costs associated with power grid operation, retrieved from grid company Elvia [56]. Many European countries adopt a price charging model similar to the one shown in Eq. (14) [57], containing fixed grid rent, tax, and variable market price; in some cases, surcharge of high peak load in winter are also included.

To analyze the impacts from different prediction models on the overall costs of the building heat supply system, a thorough study shall be carried out involving several key factors, e.g., types of HPs compressors driving force, operation optimization strategy, and sizing of the boosting HPs and water storage tank to avoid high peak surcharge. In addition to focusing heating load prediction and supply on building side, it would be interesting to examine the interactive response between DH plant/network and building user side. For example, when integrating renewables and short-to-medium-term thermal storage into LTDH, which is likely to come more in the near future, pricing models for both heat source and boosting costs shall be considered in the overall network cost optimization. Due to the length of the paper, an in-depth analysis and scenario-based projection of system cost shall be the goal of future study.

4.3. Value of transferring the developed models

There is a noticeable difference in heating load prediction performance between the model using historical heating loads and outdoor temperature as prediction inputs (g_{120}) and the models only using the outdoor temperature as inputs (the ES curve model and f_{72}), e.g. during the mild-low heating season. One reason could be the thermal inertia effects of the buildings and suboptimal control of the heating loads, which likely makes the historical heating loads be useful to model. Additionally, during this period, DHW heat use accounted for a higher

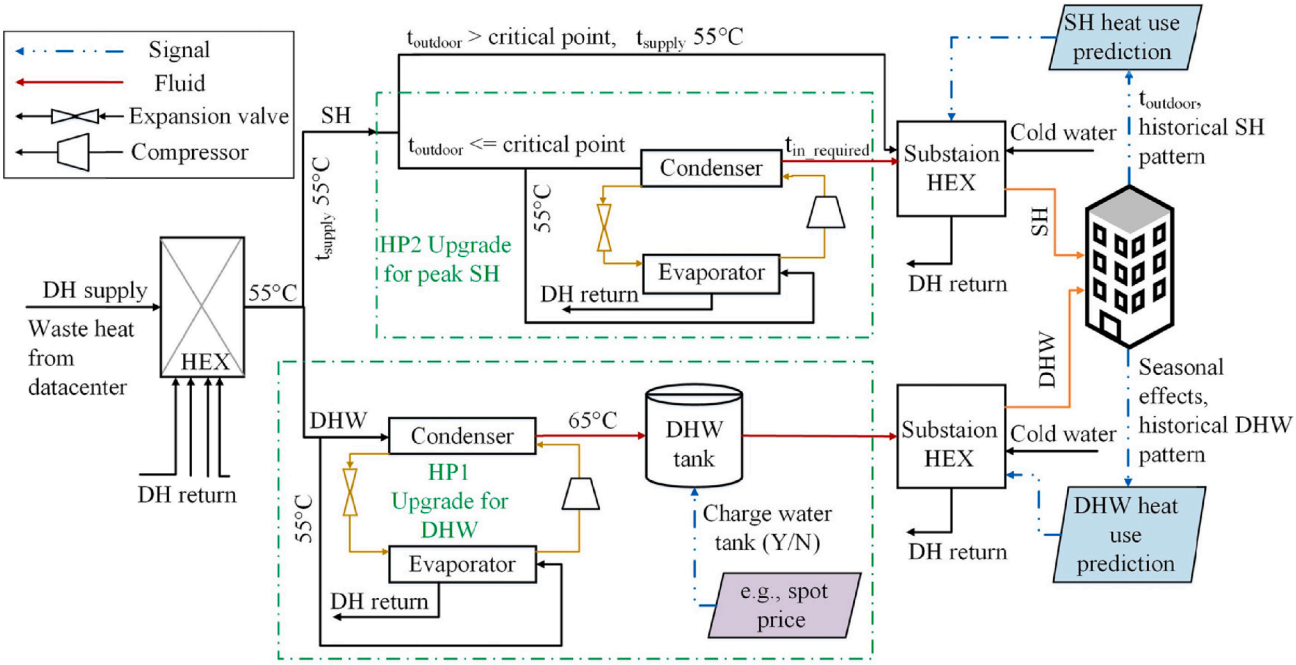

Fig. 12. Schematic diagram of integrating building-sized HPs.

share of heat demand under the weaker relationship between the outdoor temperature and the heating load. This evidence presented a basis for future LTDH transitions under different climates, that more heating loads may fall into mild-heating season and only peak loads into high-heating seasons.

Although it is important to include historical heating load for prediction models as found in the results, historical heating load data are unfortunately either accessible with delays or low data quality, i.e., low time resolution, different from historical weather data, which are usually publicly accessible via meteorological institutions. Accordingly, another potential application of the results is to map load predictions in other relevant buildings, either existing ones without high quality data collection or newly built ones with limited data for training. One of the promising methods is transfer learning (TL), which is a state-of-the-art ML technique showing excellent performance in different fields. Lately, TL has shown advantages for building energy management with adjustment of buildings' identities [58]. The gained knowledge is therefore beneficial for understanding such as newly built nursing homes or existing ones in need of renovation assessment, by transferring the developed energy prediction models of one typical building type to individual buildings.

5. Conclusions

This study proposed hybrid heating load prediction methods and examined the feasibility of integrating two building-sized HPs in an LTDH system. The work was established on the average heating load of 20 nursing homes, involving different building ages, areas, and energy labelling levels in the Nordic climate.

The main findings are as the following:

- From Method 1, the ES curve model provided a long-term heating load prediction in hourly resolution, showing a strong linear relationship between the outdoor temperature and the heating load over half of the heating seasons.
- Under the sizing boundary by Method 1, it was found to be important to include historical heating data as inputs when developing the two ANN models in Method 2, f_{72} and g_{120}. Through the accumulation of every day's day-ahead prediction, models f_{72} and g_{120} were comparable with the ES curve model on a yearly basis.
- The three models were evaluated on the actual measured data from real cases, demonstrating the feasibility of such prediction models. Among them, benefitting from considering both the historical heating load and the outdoor temperature as the inputs, the ANN model g_{120} showed the best results in the quality evaluation, especially in predicting the heating load in the mild-low heating season and peak periods.
- As one of the challenges in LTDH system, the different minimum allowable temperature requirements of DHW and SH, may be handled by integrating two building-sized heat pumps, with the respective load profiles for DHW and SH as demand inputs.

This study demonstrated hybrid building heating load prediction methods and present their possible application in building energy supply operation. The proposed methods and results were established and evaluated on a large amount of measured data and may give a better insight into building energy management and the LTDH system.

CRediT authorship contribution statement

Yiyu Ding: Conceptualization, Methodology, Data curation, Software, Formal analysis, Validation, Writing – original draft. **Thomas Ohlson Timoudas:** Methodology, Software, Validation, Writing – review & editing. **Qian Wang:** Conceptualization, Methodology, Formal analysis, Writing – review & editing. **Shuqin Chen:** Supervision, Writing – review & editing. **Helge Brattebø:** Supervision, Writing – review & editing. **Natasa Nord:** Conceptualization, Funding acquisition, Project administration, Supervision, Writing – review & editing.

Declaration of Competing Interest

The authors declare that they have no known competing financial interests or personal relationships that could have appeared to influence the work reported in this paper.

Acknowledgement

This article has been written within the research project "Methods for Transparent Energy Planning of Urban Building Stocks– ExPOSe". The authors gratefully acknowledge the main support from the Research Council of Norway (ExPOSe programme, grant number: 268248) and aided support from the Swedish Energy Agency (grant number: 51544-1). Special thanks go to the Department of Energy and Process Engineering of NTNU and Trondheim Municipality.

References

[1] U. N. Environment. 2020 global status report for buildings and construction. <https://globalabc.org/news/launched-2020-global-status-report-buildings-and-construction> [accessed Nov. 15, 2021].
[2] U. N. Environment. Global status report for buildings and construction. UNEP – UN Environment Programme, Oct. 19, 2021; 2021. <http://www.unep.org/resources/report/2021-global-status-report-buildings-and-construction> [accessed Nov. 15, 2021].
[3] European Biomass Association, EGEC geothermal, and European Solar Thermal Industry Federation. Primary energy factor for electricity in the energy efficiency directive; 2017. <http://www.estif.org/fileadmin/estif/The-role-of-PEF-in-ecodesign_AEBIOM-EGEC-ESTIF_April-2017-1_1_.pdf> [accessed Dec. 09, 2021].
[4] Latõšov E, Volkova A, Siirde A, Kurnitski J, Thalfeldt M. Primary energy factor for district heating networks in European Union member states. Energy Proc 2017; 116:69–77. https://doi.org/10.1016/j.egypro.2017.05.056.
[5] IEA. Energy policies of IEA countries: Sweden 2019 Review. IEA. <https://www.iea.org/reports/energy-policies-of-iea-countries-sweden-2019-review> [accessed Dec. 09, 2021].
[6] SSB. District heating and district cooling. SSB. <https://www.ssb.no/en/energi-og-industri/energi/statistikk/fjernvarme-og-fjernkjoling> [accessed Dec. 09, 2021].
[7] Standard Norge. NS 3700: Kriterier for passivhus og lavenergibygninger–Boligbygninger; 2013. <https://www.standard.no/no/Nettbutikk/produktkatalogen/Produktpresentasjon/?ProductID=636902> [accessed Dec. 09, 2021].
[8] Directorate of Building Quality. TEK17. Veiledning om tekniske krav til byggverk/Building Technology Regulations, Norway; 2017. <https://www.regjeringen.no/contentassets/20503ddfe0664fac9e2185c1a6c80716/veiledning-til-byggteknisk-forskrift-tek17_01_07_2017_oppdatert_15_09_2017.pdf> [accessed Dec. 09, 2021].
[9] EU Commission. Energy performance of buildings directive. <https://energy.ec.europa.eu/topics/energy-efficiency/energy-efficient-buildings/energy-performance-buildings-directive_en> [accessed Jul. 07, 2022].
[10] Averfalk H, Benakopoulos T, Best I, Dammel F, Engel C, Geyer R, et al. Low-temperature district heating implementation guidebook. IEA DHC Report; 2021. p. 206.
[11] Sorknæs P, Østergaard PA, Thellufsen JZ, Lund H, Nielsen S, Djørup S, et al. The benefits of 4th generation district heating in a 100% renewable energy system. Energy 2020;213:119030.
[12] The Research Council of Norway, "Research for Sustainable Societal and Industrial Development. <https://www.forskningsradet.no/om-forskningsradet/publikasjoner/2017/research-for-sustainable-societal-and-industrial-development/>.
[13] Buffa S, Cozzini M, D'Antoni M, Baratieri M, Fedrizzi R. 5th generation district heating and cooling systems: a review of existing cases in Europe. Renew Sustain Energy Rev 2019;104:504–22. https://doi.org/10.1016/j.rser.2018.12.059.
[14] Wang J, Cai H, You S, Zong Y, Zhang C, Træholt C. A framework for techno-economic assessment of demand-side power-to-heat solutions in low-temperature district heating. Int J Electr Power Energy Syst 2020;122:106096. https://doi.org/10.1016/j.ijepes.2020.106096.
[15] Wahlroos M, Pärssinen M, Rinne S, Syri S, Manner J. Future views on waste heat utilization – case of data centers in Northern Europe. Renew Sustain Energy Rev 2018;82:1749–64. https://doi.org/10.1016/j.rser.2017.10.058.
[16] Nord N, Løve Nielsen EK, Kauko H, Tereshchenko T. Challenges and potentials for low-temperature district heating implementation in Norway. May Energy 2018; 151:889–902. https://doi.org/10.1016/j.energy.2018.03.094.
[17] Guelpa E, Barbero G, Sciacovelli A, Verda V. Peak-shaving in district heating systems through optimal management of the thermal request of buildings. Energy Oct. 2017;137:706–14. https://doi.org/10.1016/j.energy.2017.06.107.
[18] Zhang Y, Johansson P, Kalagasidis AS. Applicability of thermal energy storage in future low-temperature district heating systems – case study using multi-scenario

analysis. Energy Convers Manage 2021;244:114518. https://doi.org/10.1016/j.enconman.2021.114518.
[19] Kauko H, Kvalsvik KH, Rohde D, Hafner A, Nord N. Dynamic modelling of local low-temperature heating grids: a case study for Norway. Energy 2017;139:289–97. https://doi.org/10.1016/j.energy.2017.07.086.
[20] Gianniou P, Liu X, Heller A, Nielsen PS, Rode C. Clustering-based analysis for residential district heating data. Energy Convers Manage 2018;165:840–50. https://doi.org/10.1016/j.enconman.2018.03.015.
[21] Talebi B, Haghighat F, Mirzaei PA. Simplified model to predict the thermal demand profile of districts. Energy Build 2017;145:213–25. https://doi.org/10.1016/j.enbuild.2017.03.062.
[22] Xue P, Jiang Y, Zhou Z, Chen X, Fang X, Liu J. Multi-step ahead forecasting of heat load in district heating systems using machine learning algorithms. Energy 2019;188:116085. https://doi.org/10.1016/j.energy.2019.116085.
[23] Debnath KB, Mourshed M. Forecasting methods in energy planning models. Renew Sustain Energy Rev 2018;88:297–325. https://doi.org/10.1016/j.rser.2018.02.002.
[24] Mohandes SR, Zhang X, Mahdiyar A. A comprehensive review on the application of artificial neural networks in building energy analysis. Neurocomputing 2019;340:55–75. https://doi.org/10.1016/j.neucom.2019.02.040.
[25] Wei Y, Xia L, Pan S, Wu J, Zhang X, Han M, et al. Prediction of occupancy level and energy consumption in office building using blind system identification and neural networks. Appl Energy 2019;240:276–94. https://doi.org/10.1016/j.apenergy.2019.02.056.
[26] Dagdougui H, Bagheri F, Le H, Dessaint L. Neural network model for short-term and very-short-term load forecasting in district buildings. Energy Build 2019;203:109408. https://doi.org/10.1016/j.enbuild.2019.109408.
[27] Lumbreras M, Garay-Martinez R, Arregi B, Martin-Escudero K, Diarce G, Raud M, et al. Data driven model for heat load prediction in buildings connected to district heating by using smart heat meters. Energy 2022;239:122318. https://doi.org/10.1016/j.energy.2021.122318.
[28] Lu Y, Tian Z, Peng P, Niu J, Li W, Zhang H. GMM clustering for heating load patterns in-depth identification and prediction model accuracy improvement of district heating system. Energy Build 2019;190:49–60. https://doi.org/10.1016/j.enbuild.2019.02.014.
[29] Song J, Zhang L, Xue G, Ma Y, Gao S, Jiang Q. Predicting hourly heating load in a district heating system based on a hybrid CNN-LSTM model. Energy Build 2021;243:110998. https://doi.org/10.1016/j.enbuild.2021.110998.
[30] Koschwitz D, Frisch J, van Treeck C. Data-driven heating and cooling load predictions for non-residential buildings based on support vector machine regression and NARX recurrent neural network: a comparative study on district scale. Energy 2018;165:134–42. https://doi.org/10.1016/j.energy.2018.09.068.
[31] Menard S. Coefficients of determination for multiple logistic regression analysis. Am Stat 2000;54(1):17–24. https://doi.org/10.1080/00031305.2000.10474502.
[32] Noussan M, Jarre M, Poggio A. Real operation data analysis on district heating load patterns. Energy 2017;129:70–8. https://doi.org/10.1016/j.energy.2017.04.079.
[33] Bai Y. A temperature control strategy to achieve low-temperature district heating in North China. Int J Sust Energy Plan Manage 2020;25:3–12. https://doi.org/10.5278/ijsepm.3392.
[34] Guelpa E, Marincioni L, Capone M, Deputato S, Verda V. Thermal load prediction in district heating systems. Energy 2019;176:693–703.
[35] Østergaard PA, Andersen AN. Booster heat pumps and central heat pumps in district heating. Appl Energy 2016;184:1374–88. https://doi.org/10.1016/j.apenergy.2016.02.144.
[36] Langseth B. Analyse av energibruk i yrkesbygg (Analysis of energy use in non-residential buildings). NVE, 2016. <https://nve.brage.unit.no/nve-xmlui/handle/11250/2488849> [accessed: Dec. 02, 2021].
[37] iEOS – Planning. <https://www2.esave.no/Esave.nsf/iEOS_Hovedbilde.xsp> [accessed Feb. 24, 2021].
[38] "Norsk Klimaservicesenter." https://seklima.met.no/observations/ (accessed Feb. 24, 2021).
[39] Enova Offentlig søk etter energiattester. <https://attest.energimerking.no/> (accessed May 10, 2021).
[40] Enova. Hensiktsmessige varme- og kjøleløsninger i bygninger (Appropriate heating and cooling solutions in buildings); 2013. [Online]. <https://www.enova.no/upload_images/380D698AC6CC4A0D98695AC29342ECDC.pdf> [accessed: Nov. 15, 2021].
[41] Ivanko D, Walnum HT, Nord N. Development and analysis of hourly DHW heat use profiles in nursing homes in Norway. Energy Build 2020;222:110070. https://doi.org/10.1016/j.enbuild.2020.110070.
[42] Østergaard PA, Andersen AN. Variable taxes promoting district heating heat pump flexibility. Energy 2021;221:119839. https://doi.org/10.1016/j.energy.2021.119839.
[43] Cai H, Ziras C, You S, Li R, Honoré K, Bindner HW. Demand side management in urban district heating networks. Appl Energy 2018;230:506–18. https://doi.org/10.1016/j.apenergy.2018.08.105.
[44] American Society of Heating Refrigerating and Air Conditioning Engineers. 2013 ASHRAE handbook: fundamentals; 2013. <http://app.knovel.com/hotlink/toc/id:kpASHRAEC1/2013-ashrae-handbook> [accessed: Feb. 27, 2021].
[45] Meade N. Industrial and business forecasting methods, Lewis, C.D., Borough Green, Sevenoaks, Kent: Butterworth, 1982. Pages: 144. J Forecast 1983;2(2):194–6. https://doi.org/10.1002/for.3980020210.
[46] Frederiksen S, Werner S. District heating and cooling. Studentlitteratur AB; 2013.
[47] Ding Y, Brattebø H, Nord N. A systematic approach for data analysis and prediction methods for annual energy profiles: an example for school buildings in Norway. Energy Build 2021;247:111160. https://doi.org/10.1016/j.enbuild.2021.111160.
[48] Lundström L, Wallin F. Heat demand profiles of energy conservation measures in buildings and their impact on a district heating system. Appl Energy 2016;161:290–9. https://doi.org/10.1016/j.apenergy.2015.10.024.
[49] Carragher M, De Rosa M, Kathirgamanathan A, Finn DP. Investment analysis of gas-turbine combined heat and power systems for commercial buildings under different climatic and market scenarios. Energy Convers Manage 2019;183:35–49. https://doi.org/10.1016/j.enconman.2018.12.086.
[50] OECD. Spending on long-term care Brief-November-2020.pdf. <https://www.oecd.org/health/health-systems. https://www.oecd.org/health/health-systems/Spending-on-long-term-care-Brief-November-2020.pdf> [accessed Dec. 02, 2021].
[51] TEK. Inneklima og legionella-Temaveiledning. Building technical regulations. <https://dibk.no/globalassets/byggeregler/tidligere_regelverk/eldre_temaveiledere_og_rundskriv/2003ho-1-legionella.pdf> [accessed Jan. 27, 2022].
[52] Ploskić A, Wang Q, Sadrizadeh S. Mapping relevant parameters for efficient operation of low-temperature heating systems in nordic single-family dwellings. Appl Sci 2018;8(10). https://doi.org/10.3390/app8101973.
[53] Li Y, Wang C, Li G, Wang J, Zhao D, Chen C. Improving operational flexibility of integrated energy system with uncertain renewable generations considering thermal inertia of buildings. Energy Convers Manage 2020;207:112526. https://doi.org/10.1016/j.enconman.2020.112526.
[54] Romanchenko D, Kensby J, Odenberger M, Johnsson F. Thermal energy storage in district heating: centralised storage vs. storage in thermal inertia of buildings. Energy Convers Manage 2018;162:26–38. https://doi.org/10.1016/j.enconman.2018.01.068.
[55] See market data for all areas. <https://www.nordpoolgroup.com/Market-data1/> [accessed Feb. 24, 2021].
[56] Elvia AS. Alt om nettleiepriser – Elvia. <https://www.elvia.no/nettleie/alt-om-nettleiepriser/> [accessed Jul. 08, 2022].
[57] Electricity price statistics – statistics explained. <https://ec.europa.eu/eurostat/statistics-explained/index.php/Electricity_price_statistics#Electricity_prices_for_non-household_consumers> [accessed Feb. 27, 2021].
[58] Fan C, Sun Y, Xiao F, Ma J, Lee D, Wang J, et al. Statistical investigations of transfer learning-based methodology for short-term building energy predictions. Appl Energy 2020;262:114499. https://doi.org/10.1016/j.apenergy.2020.114499.